Quantum Breathers in a Nonlinear Lattice

W. Z. Wang,* J. Tinka Gammel, and A. R. Bishop
Theoretical Division, Los Alamos National Laboratory, Los Alamos, New Mexico 87545

M. I. Salkola
Department of Physics & Astronomy, McMaster University, Hamilton, Ontario, Canada L8S 4M1

(Received 23 January 1996)

We study nonlinear phonon excitations in a one-dimensional quantum nonlinear lattice model using numerical exact diagonalization. We find that multiphonon bound states exist as eigenstates which are natural counterparts of breather solutions of classical nonlinear systems. In a translationally invariant system, these quantum breather states form particlelike bands and are characterized by a finite correlation length. The dynamic structure factor has significant intensity for the breather states, with a corresponding quenching of the neighboring bands of multiphonon extended states. [S0031-9007(96)00123-8]

PACS numbers: 63.20.Ry, 03.65.Ge, 11.10.Lm, 63.20.Kr

The paradigms of nonlinearity have provided numerous insights into condensed matter physics [1]. For example, the dynamics of nonlinear excitations (such as solitons, polarons, and breathers) are central to understanding thermodynamic and transport properties of various low dimensional materials [2]. As an important example of intrinsic dynamic nonlinearity, breather excitations—spatially localized and time-periodic waves in the form of bound states of linear excitations—have been found or excluded in various nonlinear models depending on the properties of nonintegrability and discreteness [3,4]. In particular, although breathers are rigorously stable in integrable partial differential equations [such as the $(1+1)$-dimensional sine-Gordon or nonlinear Schrödinger equations], they are unstable in *nonintegrable continuous* systems. Recently it has been appreciated, however, that they can be stablized, not only in integrable [5,6] but also in nonintegrable [7] cases, by *lattice discreteness* and sufficiently strong nonlinearity—in the form of dynamic localized excitations, the generalization of uncoupled oscillators. For some models, existence regimes have been rigorously established [8]. We are left with a central question for physical problems described by discrete, *nonintegrable quantum* systems: Do nonlinear solutions analogous to the classical breather exist and, if so, what are their observable signatures? This question has a long history in terms of biphonon bound states or resonances [9], and has been studied more recently in Bethe ansatz systems [10] as well as semiclassically [11]. Here, we focus on numerical exact diagonalization of a simple nonintegrable quantum anharmonic chain. We find that the classical breather solutions indeed have their quantum counterparts as eigenstates of the system Hamiltonian with distinctive signatures in appropriate correlation functions.

Our quantum nonlinear lattice model is

$$H = \hbar\Omega \sum_n \left[\frac{\hat{p}_n^2}{2} + \frac{\eta}{2}(\hat{\phi}_n - \hat{\phi}_{n+1})^2 + w\hat{\phi}_n^2 + \upsilon\hat{\phi}_n^4 \right], \tag{1}$$

with periodic boundary conditions, and with $\hat{p}_n$ and $\hat{\phi}_n$ the dimensionless canonical lattice momentum and displacement operators, $[\hat{\phi}_m, \hat{p}_n] = i\delta_{mn}$. The coefficient $\hbar\Omega$ sets the scale of energy, whereas η, w, and υ are dimensionless parameters. The first two terms describe a standard harmonic Debye lattice, while the second two terms for $w, \upsilon \geq 0$ describe a single-well ϕ^4 nonlinearity, which corresponds to the Taylor expansion of either a local nonlinear interaction due to anharmonicity or an effective lattice interaction arising from, e.g., electron-lattice coupling. Other nonlinear Hamiltonians can be treated by the same methods described below and can be expected to contain varieties of breathers. However, the simple form in Eq. (1) isolates the breather without, e.g., complications of multiply degenerate ground states. Note that the class of models represented by Eq. (1) does not conserve the total number of phonon quanta in contrast with simpler discrete quantum models where solitons have been discussed [12].

There are two limiting cases for which the physics of the model becomes transparent. First, in the absence of nonlinearity ($\upsilon = 0$), the model is trivially solvable. The linear coupling between nearest-neighbor oscillators in Eq. (1) results in spatially extended Bloch-wave states of phonons. The w term acts merely as an adjustable factor controlling the dispersion of phonon bands, and will be kept small throughout this study. Second, for $\upsilon\ (\sim 1) \gg \eta$ the ϕ^4 term plays the dominant role. However, we can again qualitatively understand many features of the system, including the appearance of breathers. The nearest-neighbor interaction governed by η will cause the local "Einstein" modes to become hybridized, creating narrow

 0031-9007/96/76(19)/3598(4)$10.00

continua of phonon states at each local vibrational energy. The ϕ^4 term produces a local repulsive interaction between two or more quanta if they are located at the same site. This interaction therefore leads to bound multiphonon states, breathers, that are split *upwards* from each multiphonon continuum [7]. These states are the simplest form of breathers we expect to find in molecular systems, i.e., whenever local nonlinear vibrations are weakly coupled to neighboring ones. Below, we consider systems with $\eta \sim \upsilon \sim 1$, which are more interesting because of their relevance to many strongly interacting solid-state systems, such as quasi-one-dimensional polymers. In this case, the nearest-neighbor Debye coupling will compete with the ϕ^4 nonlinearity to determine the correlation length of eigenstates in the system. The main physical effects of the ϕ^4 term are as follows: (i) opening finite gaps in the many-body excitation spectrum, which offers the possibility of bound states within the gaps; and (ii) suppression of the effective linear coupling, facilitating the dynamic localization of certain eigenstates.

We study this problem by numerical exact diagonalization using the Einstein phonon basis [13], where the only physical approximation is the truncation of the infinite Hilbert space. This restricts our numerical simulations to a parameter region where the nonlinearity is not too large. To maintain physical correctness and numerical reliability, we solve the problem for finite chains with moderately large nonlinearity, systematically studying the effect of truncation and system size. We adopt a modified [14] Davidson method [15] to perform the exact diagonalization for the large sparse matrix of the system Hamiltonian, and then a projective Lanczos method [16] to calculate various correlation functions. Eigenfunction convergence has been tested through the Weinstein lower bound formula [15], and the symmetries (e.g., the translational invariance under periodic boundary conditions) were also checked.

The low-lying eigenspectra for four- and eight-site nonlinear chains with representative parameter sets are shown in Fig. 1. Several characteristic features can be noted: First, as anticipated above, finite gaps are opened due to the effect of the nonlinearity υ. Second, states which originally belong to the same band in the linear Debye or Einstein lattice now split into several bands. While the nonlinearity does not allow the ordering of these bands in terms of bare phonons of the linear system, one can still roughly distinguish different bands by the bare phonon number distribution function $\rho_\alpha(m) = \langle\alpha|\delta(\sum_n b_n^\dagger b_n - m)|\alpha\rangle$ and the average number of bare phonons $\langle M_\alpha\rangle = \sum_m m\rho_\alpha(m)$, where $b_n = (\hat{\phi}_n + i\hat{p}_n)/\sqrt{2}$, and $|\alpha\rangle$ is an eigenstate of the system with crystal momentum q_α and energy ϵ_α. (We have also used this function to determine that our results are not dependent on the truncation.) In contrast to the Debye lattice, the ground state is isolated, with a finite gap to the excited eigenstates. The quantity $\rho_\alpha(m)$ for the first band above the ground state shows that it is mainly formed from one phonon state

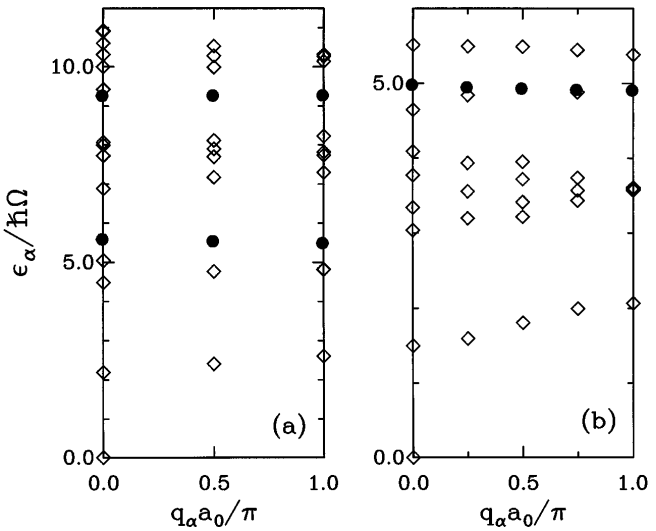

FIG. 1. Eigenspectrum of the nonlinear system: (a) four-site chain with the phonon basis truncated at 17 phonons per site (i.e., $\mathcal{M}_{\rm ph} = 18$; 65 536 states), $\eta = 0.5$, $w = 0.2$, $\upsilon = 2.0$; (b) eight-site chain with $\mathcal{M}_{\rm ph} = 6$ (1 679 616 states), $\eta = 0.5$, $w = 0.2$, $\upsilon = 0.56$. q_α labels the irreducible representation in the translation group. The dispersion is symmetric in q_α and only eigenstates with $q_\alpha \geq 0$ are shown. The solid circles denote breather states. Other states are plotted as open diamonds.

(peaked at $m = 1$). There are several different kinds of higher excited bands of states, including ones with small but finite bandwidths. The emergence of these isolated bands can be readily interpreted as the existence of particlelike states, where the bandwidth is a measure of the inverse particle mass. They can also be viewed as bound phonon states. We will argue below that these narrow, isolated bands of states are quantum breathers. Note that these breather states have explicit Bloch-wave translational symmetry with well-defined crystal momenta q_α associated with their center of mass motion. However, they also exhibit a finite lattice displacement correlation length (describing the particlelike coherence of breathers), as we now discuss.

To identify breathers in the quantum excitation spectrum, we establish their main characteristics by examining key correlation functions. These functions are not only important for diagnostic purposes, but are also relevant to many measurable quantities. One characteristic of the classical breather is spatial localization of the envelope. In the translationally invariant quantum case, the dynamic localization of breathers can be measured by the corresponding spatial correlation of the displacements at sites separated by n lattice spacings:

$$f_\alpha(n - n', t - t') = \langle\alpha|\hat{\phi}_{n'}(t')\hat{\phi}_n(t)|\alpha\rangle. \qquad (2)$$

For the linear system, these correlation functions are readily computed and in general they have multiple spatial and temporal Fourier components reflecting the system's phonon modes propagating with various phase velocities.

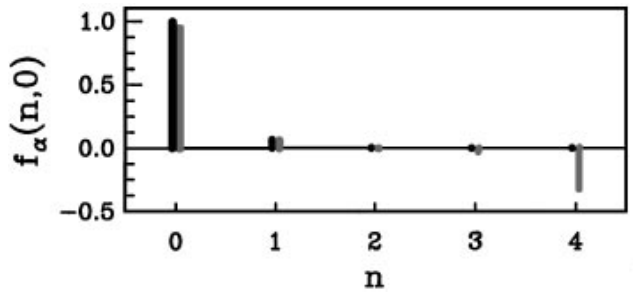

FIG. 2. The spatial correlation function $f_\alpha(n,0)$ of an eight-site system [Fig. 1(b)]: The solid line is for the lowest breather state with $q = \pi/a_0$, $\langle M_{42}\rangle = 2.83$, while the gray line is for an extended state with $q = \pi/a_0$, $\langle M_{24}\rangle = 3.13$.

However, in a nonlinear system, multiphonon bound states can appear. In Fig. 2, the instantaneous spatial correlation function $f_\alpha(n,0)$ of a typical state in the isolated bands is illustrated. The spatial correlation is clearly localized at $n = 0$ and exhibits the particlelike nature of these states, a key feature of a breather. In this strongly nonlinear regime, the breathers have a small correlation length (ξ is on the order of a lattice constant). The other states form a "continuum" of extended multiphonon states which have significant weight even at large n, also illustrated in Fig. 2.

We investigated temporal coherence in the localized state by examining the Fourier transform $F_\alpha(n,\omega)$ of the time-dependent correlation function $f_\alpha(n,t)$,

$$F_\alpha(n - n',\omega) = \sum_\beta \langle\alpha|\hat{\phi}_{n'}|\beta\rangle\langle\beta|\hat{\phi}_n|\alpha\rangle \times \delta(\hbar\omega - \epsilon_\beta + \epsilon_\alpha), \quad (3)$$

calculated using the spectral projection method [16]. $F_\alpha(0,\omega)$ for a typical breather state is shown in Fig. 3. The dynamics of the localized states exhibit a small number of frequencies with significant amplitudes, reflecting the anharmonicity of the system. The strongly localized breather here can be expected to exhibit multiple internal frequencies even classically [5,7,17], especially in the strongly nonlinear regime. However, this multifrequency property is *not* distinctive for breathers—anharmonic phonons and multiphonon states exhibit similar signatures.

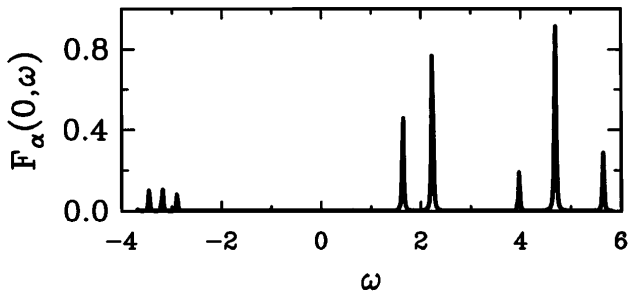

FIG. 3. The Fourier transform $F_\alpha(0,\omega)$ of the temporal correlation function for the breather state of Fig. 2. The delta-function peaks are broadened by a Lorentzian for visualization purposes.

These quantum breathers do show experimentally observable signatures of their distinctive local structure and dynamics. In particular, lattice displacements within a few correlation lengths ξ are strongly correlated in the breather and therefore can be analyzed by the density-density correlation function, $S(r,t) = (1/N)\int dr'\langle\hat{\rho}(r',0)\hat{\rho}(r'+r,t)\rangle$, where $\hat{\rho}(r,t) = \sum_n \delta(r - na_0 - \ell\hat{\phi}_n(t))$ is the density operator, a_0 is the lattice constant, N is the number of lattice sites, and $\ell = (\hbar/M\Omega)^{1/2}$ sets the scale of length for lattice displacements. The qualitative behavior of $S(r,t)$ is sensitive to the ratio r/ξ. In principle, these correlations can be probed by neutron scattering [18], which directly measures the dynamic structure factor $S(q,\omega)$ [the spatial and temporal Fourier transform of $S(r,t)$], given at zero temperature by

$$S(q,\omega) = \sum_\alpha \delta(\hbar\omega - \epsilon_\alpha + \epsilon_0)\int dr\, e^{-iqr}\int dr' \times \frac{1}{N}\langle 0|\hat{\rho}(r',0)|\alpha\rangle\langle\alpha|\hat{\rho}(r'+r,0)|0\rangle, \quad (4)$$

where $|0\rangle$ is the ground state. In the linear case, one would see a response in $S(q,\omega)$ which traces each multiphonon band dispersion, falling off exponentially in q (i.e., the quantum Debye-Waller factor) and decreasing algebraically with ω, with regular spacing in ω. The result for the nonlinear four-site system of Fig. 1(a) is illustrated in Fig. 4. The elastic response of the ground state at $\omega = 0$ has now gained an exponentially decaying q dependence which is different from the harmonic Debye-Waller factor [18]. We also note that in this zero-temperature calculation, there is no zero-frequency contribution from the breathers [19]. In addition to the expected large low-energy contributions from the ground state and the first phonon band, breather excitations are the dominant contribution, whereas those contributions from the extended multiphonon "continua" are almost negligible. The sum rule $\int d\omega\,\omega S(q,\omega) = \Omega q^2\ell^2/2$ implies that the quenching of the extended-state contribution is consistent with breathers forming as bound states of nearby phonons, and is similar to the transfer mechanism of the optical oscillator strength to local modes in the presence of electronic bound states. The center of the response is shifted to higher q for higher breather bands, consistent with the fact that higher lying breathers (binding more phonons) are narrower in the classical limit. Another clear feature of this nonlinear system revealed by $S(q,\omega)$ is that the breather bands are irregularly spaced.

To summarize, we have demonstrated that quantum breathers exist as eigenstates of the simple nonlinear lattice system studied with a renormalized mass corresponding to a narrow but finite bandwidth. The quantum breathers have been identified as robust nonlinear solutions with their own characteristic spatial localization and multifrequency dynamics. Finally, we predict that the dynamic structure factor is strongly enhanced at momentum

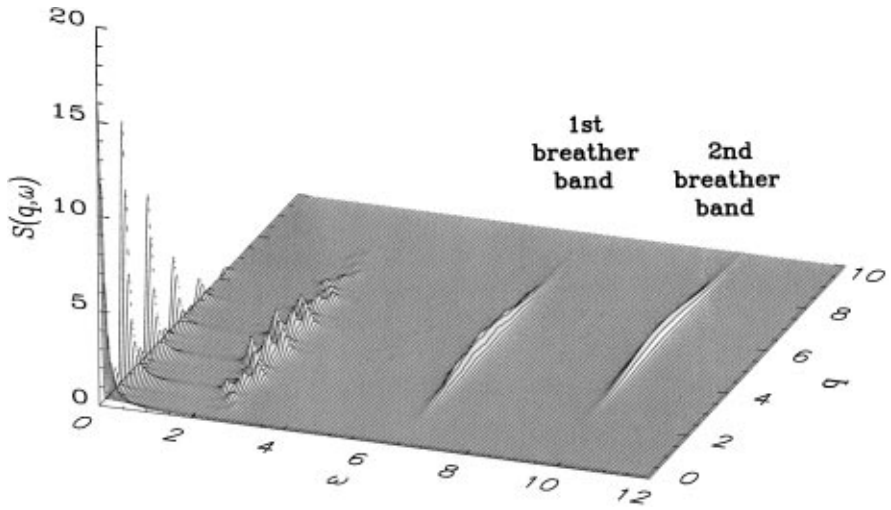

FIG. 4. The dynamic structure factor $S(q,\omega)$ of the system in Fig. 1(a) at zero temperature and $\ell = a_0/10$. Note that the equal-height δ peaks of $S(q,\omega)$ at $q = 0$ are not shown. The delta-function peaks along the ω axis are broadened by a narrow Lorentzian.

and energy transfers corresponding to breather excitations and correspondingly reduced elsewhere. This novel result should apply in more general situations and provide exciting new possibilities for the identification of breathers and other nonlinear excitations by neutron scattering. The numerical approach used here is readily applied to other nonlinear lattices and to electron-phonon coupled models, for which results will be presented elsewhere.

We thank D. Cai, S. R. White, and J. Zang for useful discussions, and E. Y. Loh, Jr., of Thinking Machines Corp. for helpful discussion. This work was performed at the Advanced Computing Laboratory of Los Alamos National Laboratory under the auspices of the U.S. Department of Energy. M. I. S. was also supported in part by Natural Sciences and Engineering Research Council of Canada, and the Ontario Center for Materials Research.

*Also at Institute for Theoretical Physics, Chinese Academy of Science, Beijing 100080, China.

[1] A. R. Bishop, J. A. Krumhansl, and S. E. Trullinger, Physica (Amsterdam) **1D**, 1 (1980).
[2] See, e.g., *Nonlinearity in Condensed Matter*, edited by A. R. Bishop *et al.* (Springer-Verlag, Berlin, 1987).
[3] For example, M. Peyrard and M. D. Kruskal, Physica (Amsterdam) **14D**, 88 (1983); D. K. Campbell and M. Peyrard, in *Chaos*, edited by D. K. Campbell (American Institute of Physics, New York, 1980), p. 305, and references therein.
[4] S. R. Phillpot, A. R. Bishop, and B. Horovitz, Phys. Rev. B **40**, 1839 (1989).
[5] D. Cai, A. R. Bishop, and N. Grønbech-Jensen, Phys. Rev. E **52**, R5784 (1995).
[6] T. Rössler and J. B. Page, Phys. Rev. B **51**, 11 382 (1994).
[7] For example, S. Takeno, in *Nonlinear Coherent Structures in Physics and Biology*, edited by K. H. Spatschek and F. G. Mertens (Plenum, New York, 1994), p. 39; S. Flach and C. R. Willis, *ibid.*, pp. 59, 63.
[8] R. S. MacKay and S. Aubry, Nonlinearity **7**, 1623 (1994).
[9] For example, J. Ruvalds, Phys. Rev. B **3**, 3556 (1971).
[10] V. E. Korepin, N. M. Bogoliubov, and A. G. Izergin, *Quantum Inverse Scattering Methods and Correlation Functions* (Cambridge University Press, Cambridge, 1993).
[11] R. F. Dashen, B. Hasslacher, and A. Neveu, Phys. Rev. D **10**, 4114 (1975).
[12] A. C. Scott, J. C. Eilbeck, and H. Gilhøj, Physica (Amsterdam) **78D**, 194 (1994).
[13] The Hamiltonian (1) can be diagonalized using different bases. We chose an Einstein basis since it is simple computationally.
[14] Rather than using the Davidson algorithm to calculate the first $\alpha \sim 200$ wave functions, we target several energies λ_k, $\epsilon_0 < \lambda_k < \epsilon_\alpha$. For each λ_k we calculate the lowest $\sim$20 eigenstates of $(H - \lambda_k)^2$, using enough λ_k to fill in the spectrum. This is computationally more efficient, yields the excited eigenstates within different energy windows, and prevents loss of states in the windows. We developed parallel algorithms on a CM-5 machine with a 2048 processor partition, and were able to find the first few hundred eigenstates of a multi-10^6 matrix in a few hours.
[15] E. R. Davidson, J. Comput. Phys. **17**, 87 (1975).
[16] E. Y. Loh, Jr. and D. K. Campbell, Synth. Met. **27**, A499 (1988); S. M. Weber-Milbrodt, J. T. Gammel, A. R. Bishop, and E. Y. Loh, Jr., Phys. Rev. B **45**, 6435 (1992).
[17] Most of the classical or semiclassical breather solutions which have been studied have a single frequency or commensurate relationship between internal frequencies in the low amplitude weakly nonlinear regime. However, incommensurate multifrequency classical breathers are also known in discrete models (Refs. [5,7]).
[18] See, e.g., M. I. Salkola, A. R. Bishop, S. A. Trugman, and J. Mustre de Leon, Phys. Rev. B **51**, 8878 (1995).
[19] W. C. Kerr, D. Baeriswyl, and A. R. Bishop, Phys. Rev. B **24**, 6566 (1981).